

Original Article

Phloem flow and sugar transport in *Ricinus communis* L. is inhibited under anoxic conditions of shoot or roots

Andreas D. Peuke^{1,2}, Arthur Gessler^{2*}, Susan Trumbore³, Carel W. Windt⁴, Natalia Homan⁵, Edo Gerkema⁵ & Henk Van As⁵

¹ADP International Plant Science Consulting, Talstraße 8, Gundelfingen D-79194, Germany, ²Institute for Landscape Biogeochemistry, Leibniz-Zentrum für Agrarlandschaftsforschung (ZALF) e.V., Eberswalderstr. 84, Müncheberg 15374, Germany, ³Max-Planck-Institute for Biogeochemistry, Beutenberg Campus, Hans-Knoell-Straße 10, Jena D-07745, Germany, ⁴IBG-2: Plant Sciences, Forschungszentrum Jülich, Leo Brandt Street 1, Jülich 52425, Germany and ⁵Laboratory of Biophysics, Wageningen University, Dreijenlaan 3, Wageningen 6703 HA, The Netherlands

ABSTRACT

Anoxic conditions should hamper the transport of sugar in the phloem, as this is an active process. The canopy is a carbohydrate source and the roots are carbohydrate sinks. By fumigating the shoot with N₂ or flooding the rhizosphere, anoxic conditions in the source or sink, respectively, were induced. Volume flow, velocity, conducting area and stationary water of the phloem were assessed by non-invasive magnetic resonance imaging (MRI) flowmetry. Carbohydrates and δ¹³C in leaves, roots and phloem saps were determined.

Following flooding, volume flow and conducting area of the phloem declined and sugar concentrations in leaves and in phloem saps slightly increased. Oligosaccharides appeared in phloem saps and after 3 d, carbon transport was reduced to 77%. Additionally, the xylem flow declined and showed finally no daily rhythm. Anoxia of the shoot resulted within minutes in a reduction of volume flow, conductive area and sucrose in the phloem sap decreased. Sugar transport dropped to below 40% by the end of the N₂ treatment. However, volume flow and phloem sap sugar tended to recover during the N₂ treatment.

Both anoxia treatments hampered sugar transport. The flow velocity remained about constant, although phloem sap sugar concentration changed during treatments. Apparently, stored starch was remobilized under anoxia.

Key-words: *Ricinus*; carbohydrates; flooding; isotopic signature; phloem; xylem.

INTRODUCTION

The primary products of photosynthesis – sugars – are translocated within plants mostly by the phloem system. The classic ‘Druckstrom-’ (pressure flow) theory (Münch 1930) divided the phloem system in three parts: loading/collection, transport and unloading/release phloem. Sugars are loaded

in the sieve tubes of the collection phloem in source tissues and unloaded/escape from the sieve tubes of the release phloem in sinks. The resulting turgor difference across the phloem drives mass flow in the source-to-sink direction (e.g. van Bel 2003; Lalonde *et al.* 2003; Gould *et al.* 2005; Pickard & Abraham-Shrauner 2009; Knoblauch & Oparka 2012; De Schepper *et al.* 2013). Along the translocation pathway – the transport phloem – sugars and water are continuously lost from and retrieved into the sieve tubes (van Bel 1993; De Schepper *et al.* 2013). Additionally, the phloem may be a pathway for signal transport (De Schepper *et al.* 2013; Turnbull & Lopez-Cobollo 2013).

In most plants, sucrose is the major osmotically active solute in the phloem and thus also provides the driving force for mass flow in the phloem (Lalonde *et al.* 2004). All plant species transport sucrose in the phloem. Some species transport detectable amounts of raffinose, stachyose and/or sugar alcohols, which can exist in even higher concentrations than sucrose (Lalonde *et al.* 2004). Next to sugars, amino N compounds and potassium largely account for phloem sap osmotic concentrations and hence pressure differences between source and sink.

In general, phloem loading and unloading can occur symplastic or apoplastic (Lalonde *et al.* 2003; De Schepper *et al.* 2013). Sucrose, and probably certain amino acids, is loaded via the apoplastic pathway into minor veins by proton symporters localized in plasma membranes of sieve element/companion cell complexes. The transport systems across the membranes are energized by proton-motive force (van Bel 2003; Lalonde *et al.* 2003; Turgeon 2010). In contrast, oligosaccharides seem to be loaded symplastically. The so-called polymer trapping involved in this loading pathway is also active from a thermodynamical point of view, although it does not involve active transport of ions or molecules across a membrane (Turgeon 2010). In the initial step, sucrose diffuses via plasmodesmata from the mesophyll into the companion cells, where raffinose and stachyose, which cannot diffuse back, are synthesized (Turgeon 2010; De Schepper *et al.* 2013). In summary, most phloem loading processes are energy dependent and therefore sensitive to conditions which hamper the synthesis of ATP, such as low oxygen concentrations. In addition to the energy demand for

Correspondence: A. D. Peuke. Fax: (0)3212-1137807; e-mail: andreas@peuke.de

*Present address: Research Unit Forest Dynamics, Swiss Federal Institute for Forest, Snow and Landscape Research WSL, Zürcherstrasse 111, CH-8903 Birmensdorf, Switzerland

loading, (1) the phloem conduits need continuous energy supply for vitality and transport activity (van Bel 2003); and (2) that even 'passive' loading requires energy in the sense that sugars accumulate only as a result of photosynthesis.

In the sink tissues, that is, at the sites of carbohydrate demand, transported sugars are unloaded from sieve elements and companion cells to the sites of utilization or storage. For phloem unloading once again, two types of mechanisms, apoplastic and symplastic, are distinguished on the basis of the cellular pathway of solute transport. For most sinks, phloem unloading follows symplastic connections. Phloem solutes are unloaded from the sieve element/companion cell complexes into arrays of sink cells connected by plasmodesmata (van Bel 2003; Lalonde *et al.* 2003). Symplastic unloading occurs in developing roots and leaves (Turgeon 1987; Lalonde *et al.* 2003). For apoplastic unloading, sugars are released from the phloem to the apoplast and are subsequently taken up across the membranes of cells in the sink tissue. This unloading type occurs in seeds or host/parasite associations. Independent of the unloading mechanism, the sugar metabolism related to growth and storage that occur after the import of photoassimilates into sink tissues are oxygen dependent.

Previous studies indicate that low external oxygen concentration can have an inhibitory effect on phloem translocation, but results are contradictory. Turgeon (1987) observed that phloem unloading in tobacco sink leaves was insensitive to anoxia. Phloem loading, transport and unloading were, however, also found to be inhibited by low O₂ concentration in other species (Thorpe & Minchin 1987; van Dongen *et al.* 2003). van Dongen *et al.* (2003) showed that oxygen concentration is generally low inside the transport phloem in *Ricinus*.

The oxygen availability in the roots may be even lower, as here the phloem is embedded in the stele. Roots often have to cope with anoxic conditions and there is no oxygen supply by photosynthesizing cells. A very common situation of anoxic stress occurs for roots if the soil is waterlogged or flooded. Plants can overcome this stress by morphological (aerenchyma, adventive roots, etc.) and biochemical reactions. It is well known that shortly after the onset of O₂ limitation, cells alter their metabolism to increase anaerobic generation of ATP by cytosolic glycolysis followed by fermentation (e.g. Tadege *et al.* 1999), a process which is, however, less efficient in generating ATP compared with respiration (Bailey-Serres & Voeselek 2008). Geigenberger (2003) observed that the rate of most biosynthetic processes decreased by more than 90% when the conditions become anoxic.

We hypothesize that phloem transport is inhibited by anoxic conditions of shoot and roots, as all steps of phloem transport, that is, loading, transport and unloading, are energy as well as oxygen dependent and thus impaired by oxygen deprivation. In order to test this hypothesis, we chose to subject the entire shoot (here in its entirety defined as source) and the entire root (sink) to anoxia, while monitoring phloem translocation by means of magnetic resonance

imaging (MRI) flowmetry and analysis of source and sink tissues as well as phloem saps. Via carbon isotopic analysis of carbohydrates, we intend to detect effects on stomatal conductance or use of stored carbon pools.

The review by Borisjuk *et al.* (2012) illustrates the potential of MRI for applications in plant science, and its potential for solving outstanding issues in plant physiology (seed and bulb development, fruit and root growth, water dynamics, stress response, host–pathogen interactions, plant metabolism, etc.). The advantages and drawbacks of utilization of this method in natural plants and crops under controlled conditions as well as in the field are shown. The rough sink-source subdivision of a *Ricinus* plant in the present study is owing to the space consuming complex MRI set-up (Peuke *et al.* 2006; Van As 2007), although parts of the shoot are still growing and therefore operating as a sink. *Ricinus* is used as a model plant since a long time *inter alia* due to ease of collecting transport saps. *Ricinus* is apoplastic phloem loading with relative large sieve tube diameter of 25–40 µm (van Bel & Kempers 1990). We detected sugar concentrations in phloem saps under different nutritional conditions between 360 and 560 mM (Peuke 2010), and the flow velocity was relative similar around 0.25 mm s⁻¹ under different conditions (Peuke *et al.* 2001; Windt *et al.* 2006). *Ricinus* seems to be sensitive against flooding because for optimal growth waterlogging should be prevented. The flow measurements were done at the hypocotyl of the plants, which represents the transport phloem. For the application of anoxia to the shoot, the ambient air around the shoot was replaced by N₂ for 3 h, whereas for inducing sink anoxia the root-soil compartment was flooded for 3 d.

MATERIALS AND METHODS

Plant material, cultivation and drought treatment period

Seeds of *Ricinus communis* L. were germinated in vermiculite moistened with 0.5 mM CaSO₄. After 13–15 d, the plants were transferred to 5 L pots with substrate consisting of two parts of commercial potting soil (Floradur; Floragard GmbH, Oldenburg, Germany) and one part of Perlite (Perligran G; Deutsche Perlite GmbH, Dortmund, Germany). Every third day, the pots were irrigated with tap water and after 1 month on substrate the plants were supplied with a commercial fertilizer (0.3% Hakaphos® Blau; Compo GmbH, Münster, Germany).

The plants were cultivated for 45–55 d in a greenhouse (26 ± 5 °C) with a 16 h photoperiod provided by natural daylight plus mercury-vapour lamps (Osram HQL 400; Osram, Munich, Germany) supplying the plant with a minimum of 300–500 µmol photons m⁻² s⁻¹ at the canopy.

Anoxia treatment of sink (root) or source (shoot)

Anoxic conditions in the root zone (sink) were imposed by flooding the plant pots with tap water (Fig. 1). The flooded plants had an axis diameter at the hypocotyl of 10.6 ± 1.6 mm

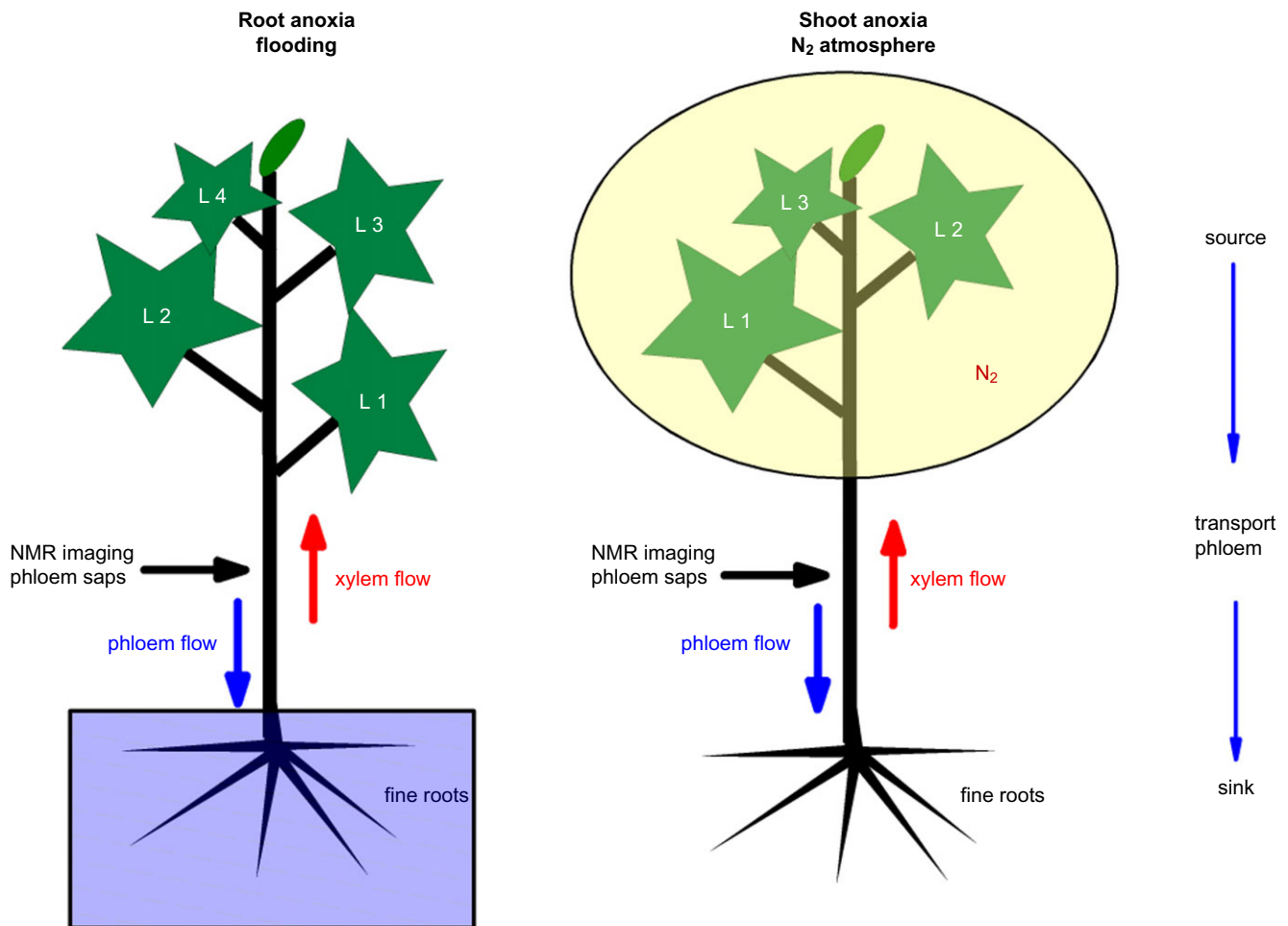


Figure 1. Experimental design and scheme of the plants used in the experiments with sampling positions. Anoxic conditions in the roots (sink tissue) were caused by flooding the plant pots with tap water. The flooded plants have had an axis diameter at the hypocotyl of around 11 mm and four intact mature leaves. For source anoxia, the entire shoots/canopy were covered with a transparent plastic bag and firstly flushed with ambient air (170 L min^{-1}) and subsequently – in order to impose anoxic conditions – with N_2 and afterwards flushed with air again. The plants for shoot anoxia treatment have had a stem diameter of around 8 mm and three mature leaves. The sampling and measurement positions are indicated.

and four intact mature leaves with an average total leaf area of $2513 \pm 435 \text{ cm}^2$.

Source anoxia was imposed by covering the entire shoot with an 80 L transparent plastic bag (Fig. 1), which was fixed below the canopy. Firstly, the plastic bag was flushed with ambient air (170 L min^{-1}) and subsequently – in order to impose anoxic conditions – with N_2 for a period of 3 h. To end the anoxic treatment, the bag was re-flushed with ambient air again. We acknowledge that complete anoxia might not be achieved by this treatment as O_2 will be produced photosynthetically. To minimize this O_2 production, we used pure N_2 (without CO_2) during the treatment. The relative humidity was monitored and kept constant at a value of approximately 70%. The plants that were selected for the shoot anoxia treatment were somewhat smaller than the plants that were subjected to flooding (stem diameter $8.2 \pm 1.4 \text{ mm}$, three mature leaves with an average total leaf area of $1638 \pm 444 \text{ cm}^2$) in order to assure a comfortable fit in the 80 L plastic bag.

Nuclear magnetic resonance (NMR) imaging set-up

The MRI system was a Bruker Advance console (Bruker, Karlsruhe, Germany) in combination with a Bruker electro-magnet (Bruker), generating a magnetic field strength of 0.72 T over a 10 cm air gap. The magnetic field was stabilized with an external ^{19}F lock unit. A shielded gradient system with a planar geometry and maximum field strength of 1 T/m (X, Y and Z directions) was used (Resonance Instruments Ltd, Witney, UK). An air gap of 50 mm between the two gradient plates provided open access from the front and back of the gradient set, as well as from above and below.

A solenoid radio frequency (RF) coil for induction and detection of the NMR signal was custom made for each individual plant. Firstly, a loosely fitting mould with a diameter of 10–12 mm was put around the stem of the plant. The RF coil was then constructed by wrapping nine turns of 0.5 mm copper wire around the mould. The finished coil was

connected to a compact, homebuilt tuning circuit, electromagnetically shielded by means of aluminium foil and copper tape, and fixed to a rod next to the plant. The assembly of pot, plant and coil was then inserted, upright, into the magnet (Peuke *et al.* 2006; Windt *et al.* 2006; Van As 2007). The environmental conditions in the magnet were 25 ± 1 °C at daytime (16 h) and 22 ± 1 °C at night-time (8 h), 20–27% relative humidity (RH) and $200 \mu\text{mol photon m}^{-2} \text{s}^{-1}$.

MRI flowmetry

Flow imaging was performed using the method described by Windt *et al.* (2006), employing a pulsed field gradient-spin echo-turbo spin echo (PFG-SE-TSE) sequence (Scheenen *et al.* 2000a). The linear displacement was measured by stepping the amplitude (G) of the PFGs from $-G_{\text{max}}$ to $+G_{\text{max}}$ and sampling q-space completely. After Fourier transformation of the signal as a function of G, the complete distribution of displacements of water in the direction of G within the labelling time Δ (called propagator, see e.g. Scheenen *et al.* 2001; Van As 2007) was obtained for every pixel in an image. From these single pixel propagators, the following flow characteristics were extracted for each volume element in the image, as described by Scheenen *et al.* (2000b): the total amount of water, the amount of stationary water, the amount of flowing water, the average linear velocity (including the direction of flow) and the volume flow. The following experimental parameters were used for phloem: image matrix 128×128 pixels, field of view (FOV) 9×9 , 11.5×11.5 or 15.5×15.5 mm depending on plant size, slice thickness 6 mm, spectral width (SW) 50 kHz, repetition time (TR) 1250 ms, two times averaging, first echo time (TE_1) 107 ms, all other echoes echo time (TE) 4.2 ms, turbo factor 8; flow encoding or labelling time Δ 100 ms (with 21 180 RF pulses during this period), with PFG duration δ 3 ms, 32 G steps, G_{max} 0.192 T/m; acquisition time 21 min 20 s. For xylem flow measurements, the experimental parameters were set as follows: image matrix 128×64 , TR 2000 ms, two times averaging, SW 50 kHz, FOV 9×9 , 11.5×11.5 or $15.5 \times 15.59 \times 9$ mm, slice thickness 3 mm; flow encoding: Δ 20 ms (with 3 180 RF pulses during this period), δ 3 ms, 32 G steps, G_{max} 0.461 T/m; acquisition time 25.

Data analysis was performed in IDL (Research Systems Inc., Boulder, Colorado, USA) using homebuilt fitting and calculation routines.

In order to construct spatially resolved phloem flow maps (amount of flowing water per pixel, average linear velocity per pixel, and volume flow per pixel), the data of at least four individual flow measurements were averaged in order to improve the signal-to-noise ratio, and then analysed on a per-pixel basis. To quantify phloem flow with a higher time resolution (one data point per individual flow measurement), the pixels containing phloem flow were identified as noted above. The propagators of these selected pixels were subsequently summed and the resulting one-dimensional total propagator was analysed to yield a quantitative flow profile of all flowing water within the phloem flow mask. Because of random diffusion, the stationary pool of water exhibited a velocity distribution that was symmetrical

around zero. The spatial resolution of both xylem and phloem flow measurements was more than sufficient to separate the pixels that contained the signal from the rapidly upward moving xylem sap, from the pixels that contained the slower downward moving phloem sap at the hypocotyl of *Ricinus*. Furthermore, the flowing xylem and phloem water were detected exactly where it was expected on the basis of anatomy.

MRI T1 and T2

T2 imaging was done using a multi spin echo imaging pulse sequence (Donker *et al.* 1997; Edzes *et al.* 1998), TR 5000 ms, a spin TE of 4.2 ms and SW 50 kHz. An image matrix of 128×64 pixels was acquired per echo, 192 echoes were acquired per echo train, 4 averages per acquisition and a TR of 2.5 s. T1 imaging was performed via saturation recovery by recording a series of 10 separate amplitude images at increasing TR (from 50 to 2500 ms), using a TSE imaging pulse sequence with slice selection (Scheenen *et al.* 2000a), 32 echoes and a turbo factor of 16, an effective TE of 4.2 ms, SW 50 kHz, eight averages and eight dummy scans. In both cases, FOV was 15×15 mm. The in-plane resolution typically was $120 \times 240 \mu\text{m}$ at a slice thickness of 3 mm. The acquired NMR data sets were processed using homemade routines written in IDL. The data sets were fitted on a per-pixel basis using a monoexponential decay function (van der Weerd *et al.* 2002), yielding quantitative maps of either amplitudes, $1/T_1$ and T_1 ; or amplitude, $1/T_2$ and T_2 (Donker *et al.* 1997; Edzes *et al.* 1998).

Collection of phloem sap and tissue samples

Phloem (sieve tube) saps were collected in parallel to MRI flowmetry from similar but independent plants (seedlings that were cultivated together with the plants for the MRI flowmetry experiments with same age, biomass, number of leaves and size) by shallow incisions into the bark of the hypocotyl (Fig. 1). The environmental conditions during sap collection were the same as in NMR experiments. Sap samples were collected within 15 min intervals according to Pate *et al.* (1974) and Jeschke & Pate (1991), transferred with a capillary into a 1.5 mL reaction tube and frozen immediately.

In addition, discs from mature fully expanded leaves (three to four leaves, Fig. 1) were taken and fine root samples were harvested and frozen in liquid nitrogen for the assessment of sugars, starch and $\delta^{13}\text{C}$ in total and water soluble organic matter. Before further analysis, the tissue materials were lyophilized.

Extraction of different carbon compounds

All tissue samples were homogenized in liquid nitrogen. For the extraction of water soluble organic matter, 1.5 mL of deionized water was added to 0.1 g aliquots of plant material. The mixture was agitated for 1 h at 4 °C and then the extract was boiled at 100 °C for 1 min to precipitate proteins and

centrifuged (12 000 *g* for 5 min at 4 °C). Richter *et al.* (2009) showed that extraction with distilled water gained concentrations for individual sugars comparable to ethanol or methanol extractions and that post-extraction heating did not considerably affect carbohydrate concentrations in extracts. Any change in sugar concentration as a result of a potential activity of sugar-hydrolysing enzymes during extraction in pure water is thus assumed to be negligible at the low temperatures applied here.

Determination of starch was performed after methanol/chloroform/water extraction followed by an enzyme hydrolysis modifying the method described by Wanek *et al.* (2001) and Göttlicher *et al.* (2006).

Determination of sugar concentrations in phloem saps and tissue extracts

For the determination of soluble carbohydrates, 100 μ L aliquots of diluted phloem saps, extracts from aqueous extraction and starch digestion were injected into a Dionex DX 500 HPLC-system (Dionex, Idstein, Germany). Separation of sugars was achieved on a CarboPac 1 separation column (250 \times 4.1 mm; Dionex) with 36 mM NaOH as an eluent at a flow rate of 1 mL min⁻¹. Carbohydrates were measured by means of a pulsed amperometric detector equipped with an Au working electrode (Dionex DX 500; Dionex). Individual carbohydrates that eluted 8–16 min after injection were identified and quantified by internal and external standards.

Isotope measurements and isotopic calculations

Carbon isotope signatures and carbon contents of oven-dried bulk plant material, the dried water soluble tissue extracts and phloem saps were determined using a Delta V advantage IRMS (ThermoFisher, Bremen, Germany) coupled to an elemental analyser (Flash EA; ThermoFisher) as described in detail by Keitel *et al.* (2006) and Brandes *et al.* (2006). The samples, which were combusted in tin capsules (IVA Analysentechnik, Meerbusch, Germany), contained on average between 200 and 400 μ g organic C. Carbon isotope signatures ($\delta^{13}\text{C}$ in ‰) are presented as the ratios of ¹³C/¹²C of a sample relative to the Vienna Pee Dee Belemnite standard (VPDB).

Statistics

The NMR imaging experiments were repeated at least three times with different plant individuals. Chemical analyses were made on five to six individual plants.

All statistical calculations were performed with SAS release 9.2. One-way analyses of variance [ANOVAS, model: 'time (of sample collection)'] were performed by the procedure general linear model (GLM). The adjustment of multiple comparisons according to Tukey was chosen for the *P*-values and confidence limit for the differences of least squares means (LS means).

RESULTS

Root anoxia – the flooding experiment

Flows and water relations

After the start of the flooding treatment, the volume flow in the phloem of *Ricinus* declined slowly from -0.16 ± 0.02 mm³ s⁻¹ ('-' relates to basipetal transport, as opposed to '+' for acropetal transport in the xylem) during the first day of monitoring to -0.10 ± 0.01 mm³ s⁻¹ after 2 d and remained at this level until the end of the experiment (Fig. 2a). Similarly, the flow conducting area of the phloem was reduced from 0.54 ± 0.09 mm² during the first day after flooding to 0.32 ± 0.06 mm² on days 3–4 following flooding (Fig. 2c). In contrast, the linear velocity of phloem flow remained nearly unaffected by the flooding treatment and was on average -0.27 ± 0.06 mm s⁻¹ throughout the whole experimental period (Fig. 2b). A slight reduction of stationary water in the phloem area from 7.76 ± 0.51 to 6.71 ± 0.56 mm³ was observed during the flooding treatment (Fig. 2d).

The typical daily time course of xylem mass flow, with high flow rates during the light period and much lower rates in the dark, was suppressed by the flooding treatment. At the beginning of flooding at midday of day 0, the volume flow in the xylem was approximately 4 mm³ s⁻¹, the linear velocity was 2.2 mm s⁻¹, and the flow conducting area was 2 mm² (Fig. 3a–c). In the subsequent dark period, the values of these parameters dropped to 1 mm³ s⁻¹, 0.7 mm s⁻¹ and 1 mm², respectively. After the onset of light on day 1 after flooding, volume flow, velocity and conducting area started to increase again, but dropped before midday and did not reach the maximum values of the day before. On the second day after flooding, only a slight increase in volume flow and velocity was observed immediately after the light was switched on, but this increase was followed by a drop to constantly low values until the end of the experiment (Fig. 3). The xylem volume flow remained at 0.41 ± 0.16 mm³ s⁻¹ after 2 d, the linear velocity reached 1.01 ± 0.41 mm s⁻¹ only, and the xylem flow conducting area was 0.41 ± 0.13 mm². Furthermore, the stationary water in the xylem was reduced from 26.2 (day 0) to 19.2 ± 1.9 mm³ (day 3) as a result of flooding (Fig. 3d).

From the amplitude, T1 and T2 maps (Fig. 4), we can clearly conclude that the decline in flow conducting area is not due to xylem cavitation. Although the amount of water in the secondary xylem region decreased, the xylem vessels can still be observed as high-intensity dots in the amplitude, T2 and T1 maps, and thus are still filled with water. The 1/T2 and 1/T1 maps revealed a decrease in (short) relaxation times in the xylem tissue surrounding the vessels (background in the images). A clear decrease in T1 and T2 of the pith was observed, but the amplitude of the pith did not change systematically. Only a minor decrease was observed in the amplitude in the secondary (and primary) phloem and the cortex. T1 and T2 of these tissues tended to decrease, as can be observed from the increase in the 1/T1 and 1/T2 maps. Interestingly, the bright T1 and T2 ring in-between the secondary xylem and secondary phloem (vascular cambium) is only part of the bright ring in the amplitude map (see red line for comparison). That bright amplitude ring covers outer xylem, cambium and

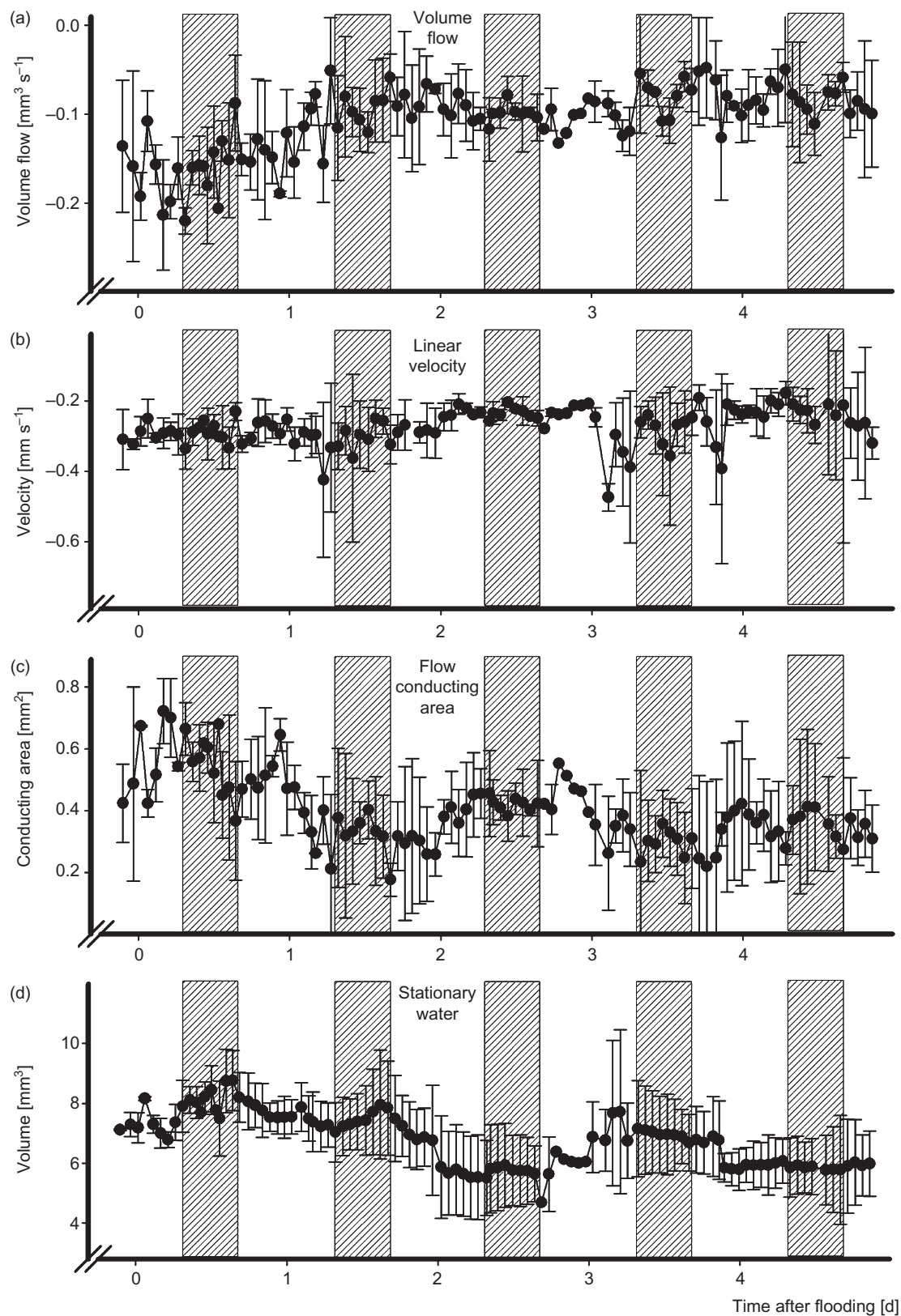


Figure 2. Volume flow (a), average linear flow velocity (b), flow conducting area (c) and stationary water (d) in the transport phloem of 45- to 55-day-old *Ricinus communis* under (root) flooding conditions (start at time point 0), measured at the hypocotyl by means of nuclear magnetic resonance (NMR) flow imaging. The grey columns are indicating the dark period. Measurements were repeated with three different plants, standard deviations are indicated by the error bars.

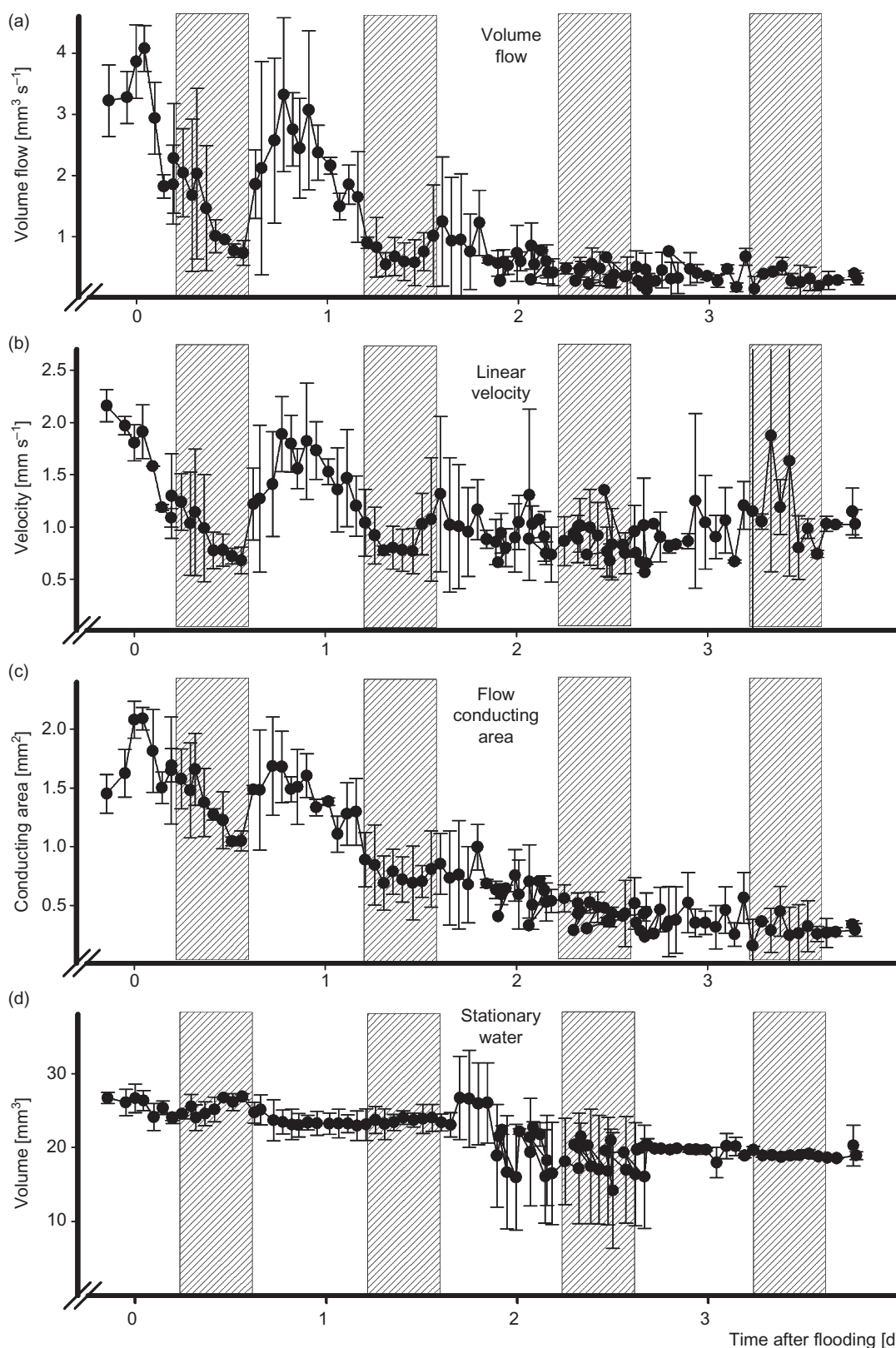


Figure 3. Volume flow (a), average linear flow velocity (b), flow conducting area (c) and stationary water (d) in xylem of 45- to 55-day-old *Ricinus communis* under (root) flooding conditions (start at time point 0), measured at the hypocotyl by means of nuclear magnetic resonance (NMR) flow imaging. The grey columns are indicating the dark period. Measurements were repeated with three different plants, standard deviations are indicated by error bars.

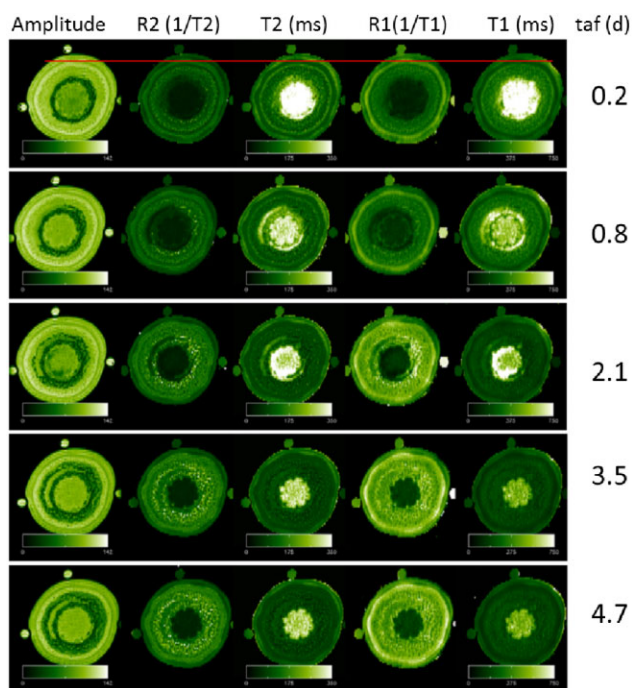


Figure 4. Amplitude, $1/T_2$, T_2 , $1/T_1$ and T_1 maps as a result of MSE MRI experiments on the stem of one of the *Ricinus* plants as a function of the time after flooding (taf) during a flooding experiment. For the position of phloem and xylem, please see Fig. 1 in Peuke *et al.* (2001).

inner phloem tissue. The T_1 and T_2 values of the bright relaxation ring decreased during flooding and can hardly be observed in the relaxation maps already after 2 d of flooding.

Carbohydrates

Sugar concentration increased in phloem saps following flooding (Fig. 5a) with sucrose always being the dominant sugar (155 ± 19 mM control/before starting the flooding treatment). Sucrose concentrations increased after 1 d of flooding to 119% of initial values and to around 130% at days 2 and 3. Raffinose, which was close to the detection limit in untreated plants, increased by a factor of 10 until day 3. Two days after starting the flooding treatment, stachyose was detected for the first time in phloem saps and amounted to 0.78 ± 0.38 mM after 3 d. $\delta^{13}\text{C}$ in phloem sap organic matter (Fig. 5b) and water extracts of leaf material (data not shown) was not affected by the flooding treatment.

Sugar concentrations in leaf material increased continuously over the experimental period and reached finally 170% (glucose), 190% (fructose) and 325% (sucrose) of the values before flooding (Fig. 5d). In roots, in contrast, glucose (38% of the initial value) and fructose (57%) decreased significantly by trend following flooding, while sucrose (332%) increased – even though not significantly – to an extent similar to leaves (Fig. 5e). In roots, flooding did not affect $\delta^{13}\text{C}$ of the bulk fraction, but $\delta^{13}\text{C}$ in the water soluble fraction increased by 1.6%. Root starch concentration increased to 140% of the initial value after 3 d of flooding (Fig. 5f).

Shoot anoxia – the shoot N_2 exposure experiment

Phloem flows

Within minutes after starting the N_2 treatment, volume flow and conducting area of the phloem started to drop. These remained at low values until 2 h after the start of the treatment (Fig. 6a,c), while the linear velocity stayed relatively constant over the entire duration of the N_2 treatment (Fig. 6b). Already during the course of the N_2 treatment, and thus before the end of the anoxia treatment, volume flow and flow conducting area of phloem started to increase again, but did not fully recover to the initial values during the observation period. The stationary water in the phloem increased after starting the N_2 treatment, but due to the high standard deviations of the mean values the change was not significant (Fig. 6d).

Carbohydrates

Refractometer measurements of phloem sap showed that total solute concentration (mainly sugars) dropped within 15 min after the start of the treatment, to 85% of the initial values (Fig. 7a). After the end of the treatment, sugar concentration increased slowly. The detailed analysis of the sugar composition in the phloem sap showed that sucrose dropped from 178 ± 39 mM to 144 ± 20 mM in the middle of the N_2 treatment followed by a slight recovery to 154 ± 37 mM at the last sampling time (Fig. 7b). Glucose and fructose concentrations were negligible in phloem sap and did not reach values higher than 5 mM (data not shown). The $\delta^{13}\text{C}$ in phloem sap increased owing to the shoot anoxia conditions from values of $-29.4 \pm 0.7\text{‰}$ at the start of the N_2 treatment to values between -27.4 and -27.0‰ at the end (Fig. 7c).

In the source leaves, glucose [138 ± 35 $\mu\text{mol g}^{-1}$ DW (dry weight)] and fructose (133 ± 26 $\mu\text{mol g}^{-1}$ DW) concentrations were similar at the start of the N_2 treatment, while sucrose was remarkably lower (15.4 ± 9.0 $\mu\text{mol g}^{-1}$ DW) (Fig. 7d, start). Under shoot anoxia conditions, concentrations of all sugars detected dropped similarly to approximately 50% of the initial concentrations after 3 h of the N_2 treatment. They subsequently recovered to ~70% of the initial values at the last sampling point 3.5 h after end of the N_2 treatment. In parallel to the sugar decrease in leaves, the leaf starch concentration was reduced from 19.2 ± 14.2 $\mu\text{equival. g}^{-1}$ DW at the beginning of the treatment to 57 or 67% at the end of the treatment and after recovery (Fig. 7e).

DISCUSSION

Sink anoxia – effects of flooding on phloem and xylem flow

The flooding treatment reduced the phloem mass flow after around 1 d, which seemed to be caused by a reduction of the conducting area (i.e. by a reduced number of active sieve tubes). The sugars in the phloem sap and source leaves accumulated apparently as a consequence of diminished export and inhibited consumption of carbohydrates in the roots under anoxia. In the phloem sap, not only did sucrose

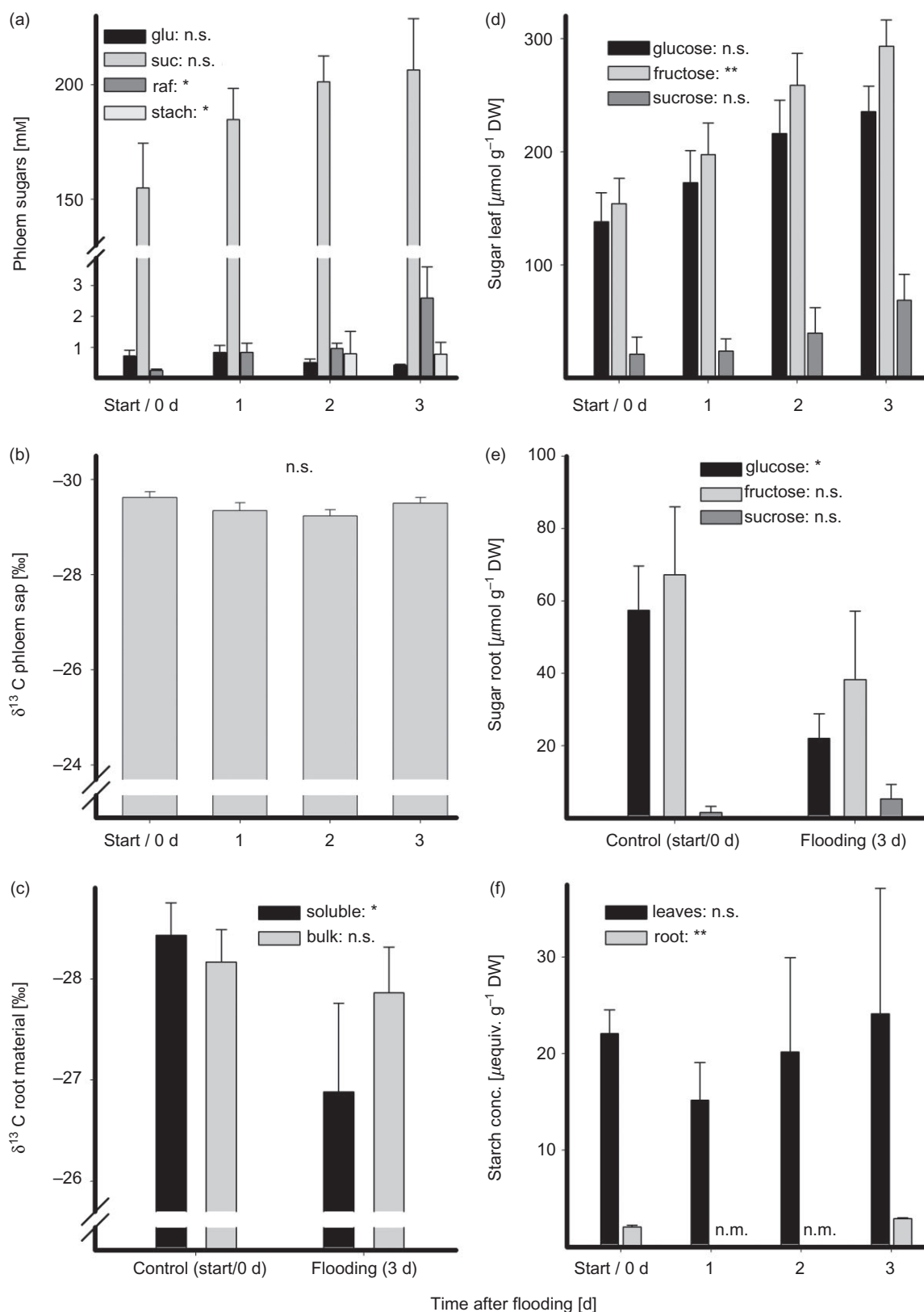


Figure 5. Carbohydrates in phloem saps, source leaves and roots of 45- to 55-day-old *Ricinus communis* following flooding: (a) glucose, sucrose, raffinose and stachyose in phloem saps collected at midday; (b) $\delta^{13}\text{C}$ of phloem saps; (c) $\delta^{13}\text{C}$ in bulk material and soluble fractions of control roots and after 3 d of flooding; (d) glucose, fructose and sucrose in source leaves; (e) glucose, fructose and sucrose in control roots and after 3 d of flooding; and (f) starch in leaves and roots.

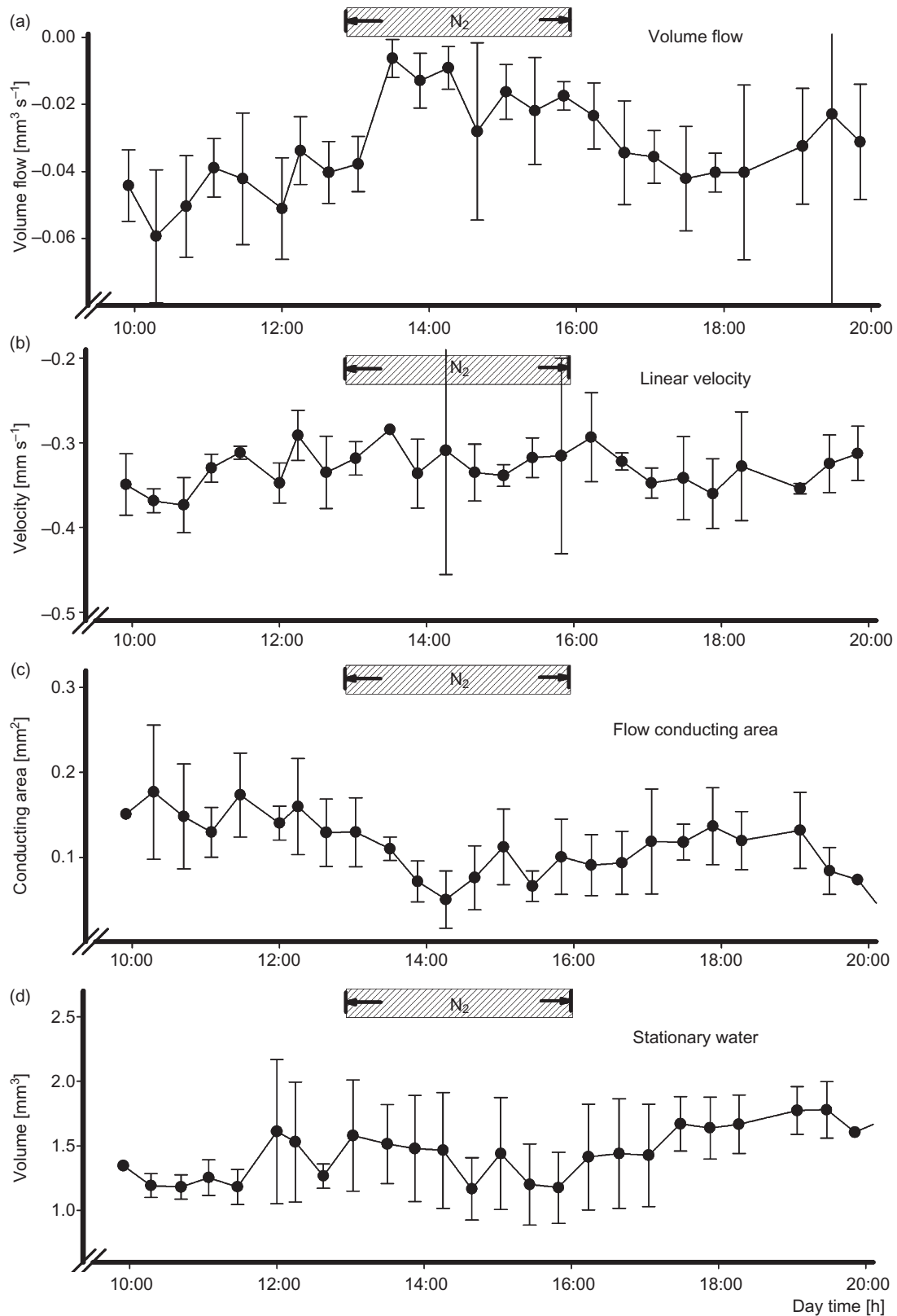


Figure 6. Volume flow (a), average linear flow velocity (b), flow conducting area (c) and stationary water (d) in the transport phloem of 45- to 55-day-old *Ricinus communis*, measured at the hypocotyl by means of nuclear magnetic resonance (NMR) flow imaging. Between 1200 and 1500 h, the ambient atmosphere around the shoot was exchanged by N₂ (shoot anoxia). Measurements were repeated with three different plants, standard deviations are indicated by error bars.

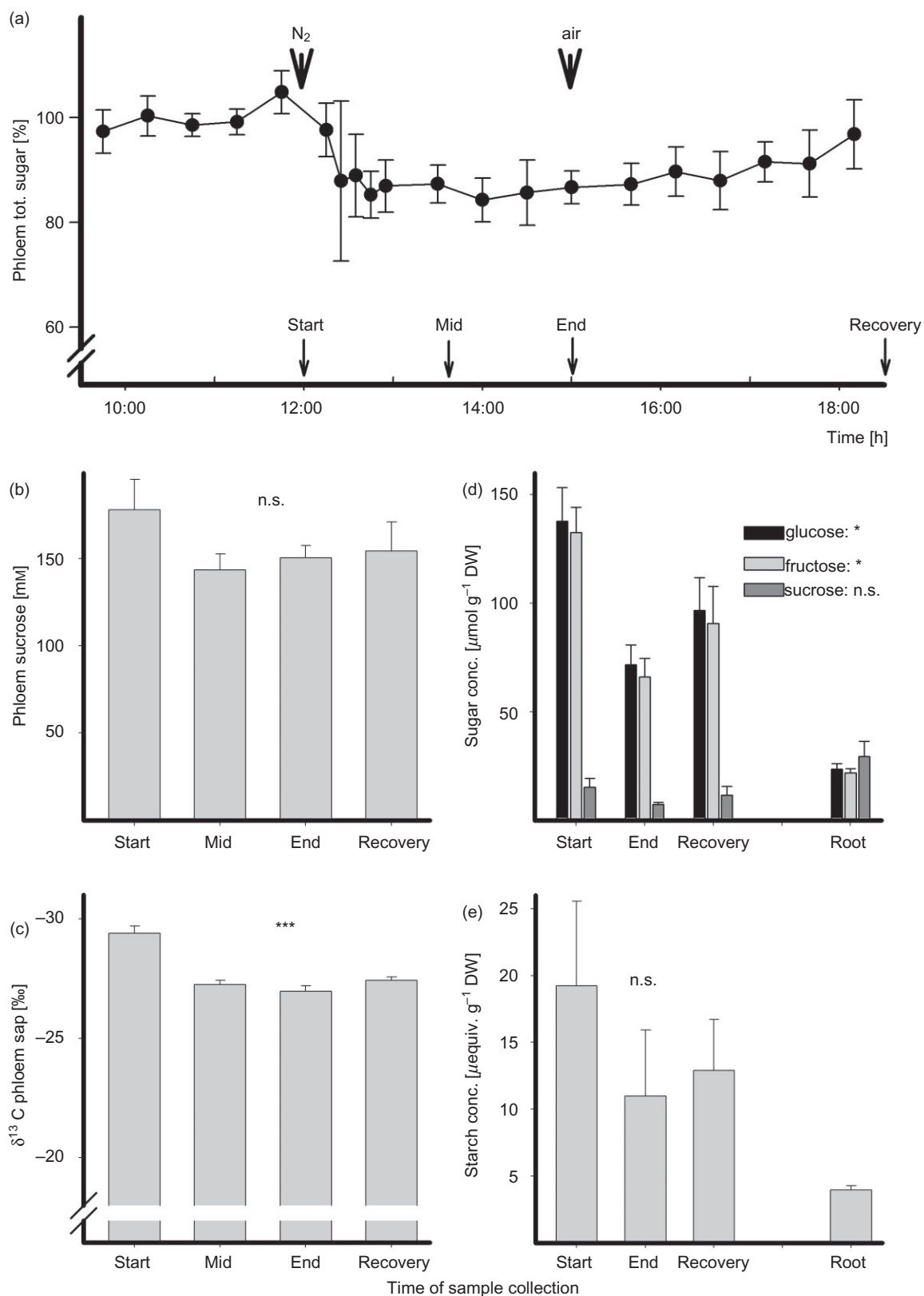


Figure 7. Carbohydrates in phloem saps, source leaves and roots of 45- to 55-day-old *Ricinus communis* before, during and after N₂ treatment of the shoot (shoot anoxia): (a) sugar concentration in phloem saps by refractometer measurements, 100% sucrose (before N₂ treatment) representing $8.10 \pm 1.07\%$ (W/V) = 244 mM; (b) sucrose in phloem saps; (c) $\delta^{13}\text{C}$ of phloem saps; (d) glucose, fructose and sucrose in source leaves and roots; (e) starch in source leaves and roots (after N₂ treatment). Data shown are means of 5–9 replicates \pm SE.

increase, but oligosaccharides also appeared. These indicate the activation of an additional phloem loading mechanism: polymer trapping. The isotopic composition of the transported sugars was not affected and therefore points to a more or less unaffected use of current photosynthates. An increased proportion of starch-derived sugars would have caused an increase in $\delta^{13}\text{C}$ as starch is ^{13}C enriched compared with sugars directly derived from 3-phosphoglycerate (e.g. Gessler *et al.* 2008), and the lack of such an increased starch remobilization is in agreement with the unchanged leaf starch concentration. In contrast, the roots became depleted in carbohydrates in the present study.

In nature, plant roots do not face anoxic conditions suddenly, but rather in a transition that occurs over a period of at least hours or even days (Gharbi *et al.* 2009), while the available oxygen in the waterlogged soil is continuously consumed by plant roots and microorganisms. In the present study, the first effects on phloem and xylem were observed after approximately 1 d, but it took more than 2 d until more or less stable and very low transport rates in both systems, particularly in the xylem, were detected.

In case of reduced availability of O_2 , the final electron acceptor in the mitochondrial electron transport chain becomes limiting, which results in a rapid reduction of the cellular ATP : ADP ratio (Bailey-Serres & Voeselek 2008). Instead of respiration, plant roots start to rely on cytosolic glycolysis and fermentation of pyruvate to ethanol or lactate for generation of ATP and regenerate NAD^+ , respectively (e.g. Tadege *et al.* 1999; Jaeger *et al.* 2009; Narsai *et al.* 2011). Fermentation is, however, less effective in production of ATP than respiration and leads finally to an energy crisis (Bailey-Serres & Voeselek 2008).

In addition to this well-known, less efficient utilization of carbohydrates under flooding, our results indicate a reduced transport of new carbohydrates to the roots. A unique aspect of this study is the ability to reliably estimate sugar transport in phloem through combined measurements of sugar concentrations and phloem volume flow. Our data demonstrate that flooding reduced carbohydrate transport in the phloem to below 80% of pre-flooding values after 3 d. Although the amount of total sugar carbon increased to 136% after 3 d of flooding, the volume flow in the phloem dropped to only 54% over the same time period, and thus overcompensated for the concentration increase. The reduced carbohydrate transport, together with the less efficient energy conversion of fermentation, could ultimately result in carbon starvation in the root of the flooded plants, as indicated by the reduced root sugar concentrations (in total 56% of control).

Surprisingly, the increase of total sugar content had no effect on the phloem velocity. This is in agreement with the several observations with different plant species indicating that phloem velocity is remarkably constant as observed in some plants (e.g. Windt *et al.* 2006; Mullendore *et al.* 2010) and in *Ricinus* subjected to different conditions like light/dark (Peuke *et al.* 2001; Windt *et al.* 2006) or cold temperature (Peuke *et al.* 2006). The increased total sugar concentration will, however, result in an increase in viscosity which is assumed to reduce hydraulic conductivity and thus phloem velocity (Thompson & Holbrook

2003). Jensen *et al.* (2011) argued that mainly for very narrow sieve tubes, resistance in the tube will determine flow velocity and consequently under these conditions changes in viscosity will be effective. In the present study, the sucrose concentrations in phloem saps changed between 155 and 206 mM (flooding) or 144 and 178 mM (shoot anoxia), respectively. In this concentration range, the effect on the viscosity is relatively low (see Fig. 2 in Hall & Minchin 2013).

The effects of flooding and related anoxia on the carbohydrate concentrations in roots are generally well studied, but results are contradicting showing increases as well as decreases. However, the duration of the treatment in each study was very different. For example, Gharbi *et al.* (2009) showed that sugar concentrations in roots increased after 1 week of hypoxic treatment in tomato. In poplar roots, starch and sucrose degradation was altered under hypoxia increasing the availability of carbohydrates (Kreuzwieser *et al.* 2009). At the same time, sucrose concentrations in the leaves decreased whereas sucrose concentrations were elevated in the phloem. Comparably, carbohydrate concentrations increased in roots of *Fraxinus angustifolia* and in a flooding-tolerant provenance of *F. excelsior* upon anoxia (Jaeger *et al.* 2009). In contrast, root carbohydrate concentrations were unaffected by flooding in another (less flooding adapted) *F. excelsior* provenance (Jaeger *et al.* 2009) and decreased sugar concentrations were also observed in other tree species (Vu & Yelenosky 1991; Angelov *et al.* 1996). One important shortcoming of recent studies is the lack of information as to whether changes in root carbohydrate concentrations are due to altered phloem transport. Jaeger *et al.* (2009) observed increased concentrations of phloem sugars upon flooding in all three species/provenances but not necessarily changes in root carbohydrate concentrations. Our example shows that phloem sugar concentrations are not necessarily indicative for phloem sugar transport, because only the combination with volume flow indicates the transport.

Sucrose is the dominant sugar transported in the phloem in most plant species. However, plants can translocate several forms of carbohydrates in addition to sucrose, such as sorbitol, mannitol and members of the raffinose family like stachyose (Slewiniski & Braun 2010; Turgeon 2010). For loading of raffinose and stachyose into the phloem, a third mechanism exists in addition to symplastic and apoplastic: polymer trapping, a symplastic but active process. Polymer trapping is similar to symplastic loading; however, an energy-requiring process is included. In our experiment, where sugars accumulate in leaves of flooded *Ricinus* plants, sucrose conversion to raffinose or stachyose increases the total concentration of sugars in the phloem sap.

Similar to our results, raffinose concentrations also increased in the phloem sap and in leaves of potted 4-month-old eucalyptus plants following 2 weeks of flooding (Merchant *et al.* 2010). Komor (2000) described the coexistence of several loading systems and that the contribution of each may be modulated by environmental factors. Together, the results show that the mechanisms and loading pathways are flexible as postulated by Rennie & Turgeon (2009).

Accumulation of toxic products such as ethanol, acetaldehyde and lactate during fermentation leads to a decrease of

cellular pH (Shabala 2011) and can cause cell death in roots and injury to shoots by transport via xylem during flooding. Flooding also affects chemical conditions in the soil. The main form of nitrogen available for plants in flooded soils is ammonium (Shabala 2011), which has been demonstrated to be less beneficial compared with nitrate and even to be toxic in *Ricinus* (Peuke & Jeschke 1993). Additionally, phytotoxic inorganic organic substances can accumulate in soils with low oxygen (Shabala 2011).

The xylem flow decreased due to the flooding treatment as well in the present study. Already after the first day of flooding volume flow, velocity and conducting area in the xylem were clearly inhibited. At the end of the flooding treatment, the diurnal rhythm of xylem transport was totally missing. A very fast response of plants to anoxia stresses is down-regulation of water uptake due to inhibition of the water permeability of roots. Else *et al.* (2008) attributed the initial stomatal closure of *Ricinus* upon flooding to decreased leaf hydration arising from the reduced hydraulic conductance of oxygen-deficient roots. Tournaire-Roux *et al.* (2003) explained the inhibition of water uptake by aquaporins gating by cytosol acidosis due to anoxia. There was no evidence for xylem cavitation (Fig. 4). The observed decrease in T1 and T2 of xylem tissue surrounding the vessels and of the vascular cambium in the shoot may point to an increased permeability to facilitate radial transport (van der Weerd *et al.* 2002) or injury (leakage of cells) due to toxic products (Donker & Van As 1999). The combination of decrease of amount of water in the xylem pool and its relaxation times indicates cell injury/death to be most likely and/or points to the function as a storage reservoir to avoid xylem cavitation.

Source anoxia – effects of shoot anoxia on phloem flow

Within minutes after starting the shoot anoxia treatment by replacing the ambient air with N₂, the volume flow in the phloem was reduced to nearly zero (due to reduced conducting area) and the sugar concentration decreased simultaneously. Shortly after this sharp inhibition, phloem flow as well as phloem sugar concentration started to recover, even as the treatment continued. After removing the N₂ atmosphere, the volume flow and sugar concentration in the phloem sap began to recover, and continued to increase until the end of the experiment. During the whole experiment, phloem velocity remained constant, despite the changes in total sugar content and accompanied viscosity.

Previously, we observed that phloem flow continued after the onset of darkness (Peuke *et al.* 2001). Regarding the availability of current photosynthates, this situation is similar to a shoot in CO₂-free N₂ atmosphere where photosynthetic C assimilation does not operate. Apparently, stored starch tended to degrade (Fig. 7e) under shoot anoxia. These starch-derived sugars are exported to the phloem (indicated by the less negative $\delta^{13}\text{C}$ of the phloem carbohydrates) to maintain transport to sink tissues. It is surprising that leaves export carbohydrates under such conditions even though CO₂ is not

being fixed and considering the fact that the supply of energy for sugar loading is strongly reduced due to anoxia.

It is well known that after a short time under O₂ limiting conditions, cells alter their metabolism to fermentation (Bailey-Serres & Voesenek 2008). However, cytosolic glycolysis is inefficient, yielding 2–4 mol ATP per mol hexose as compared with 30–36 mol ATP in mitochondrial respiration. In our study, sucrose concentration was halved (as well as glucose and fructose) after 3 h anoxia in *Ricinus* leaves. The decrease of leaf starch and the less negative $\delta^{13}\text{C}$ values in the phloem sap in the present study additionally point to the degradation of starch during shoot anoxia treatment and loading of resulting sugars into the phloem. Bailey-Serres & Voesenek (2008) observed that starch was converted to glucose due to the induction of amylases by low O₂, a finding that is supported by our results.

Thorpe & Minchin (1987) observed that phloem loading decreased under anoxia in C3 leaves, but not in general in the leaves of either C4 monocots or dicots in the light. Turgeon (1987) showed that phloem import in a sink leaf was inhibited by anaerobic conditions of a source leaf. On the other hand, phloem unloading continued if the sink leaf was exposed to a N₂ atmosphere. The findings by Turgeon (1987) were consistent with active phloem loading, but passive symplastic sugar transport from phloem to neighbouring tissue. Because of low oxygen availability, a number of biosynthetic activities decrease to less than 10% of rates at ambient oxygen (Geigenberger 2003).

Overall, the present observations with a strong decrease of phloem volume flow and sugar concentrations directly after imposing anaerobiosis and a recovery already during the N₂ treatment point not to a direct inhibition of phloem flow, but to a switch from loading of current photoassimilates to the use and degradation of starch for phloem transport.

CONCLUSION

Both anoxic treatments affected the phloem flow, but not the phloem velocity (Fig. 8). Flooding (sink anoxia) resulted in a slow effect on phloem transport and no signs of recovery during the treatment. The slow onset of the effects can be explained by the slow oxygen consumption and depletion during this treatment. Phloem flow was reduced; carbohydrates accumulated in leaves and phloem, but were depleted in roots. Phloem loading strategy shifted apparently during the flooding experiment by inducing additional oligosaccharide trapping to accumulate more reduced C in phloem saps. In contrast, during shoot anoxia (source anoxia), the phloem transport reaction was fast but recovered already during the stress. The carbohydrate analysis pointed to remobilization of starch for loading and keeping the phloem active. In both experiments, the sugar transport in the phloem was decreased, although in the case of flooding the sugar concentration in the phloem increased.

In both cases – in the shoot as well as in the root – the induction of anoxia is a problem, because the phloem is deeply embedded into other tissues. Next to the problem of causing anoxia in the loading or unloading phloem, other

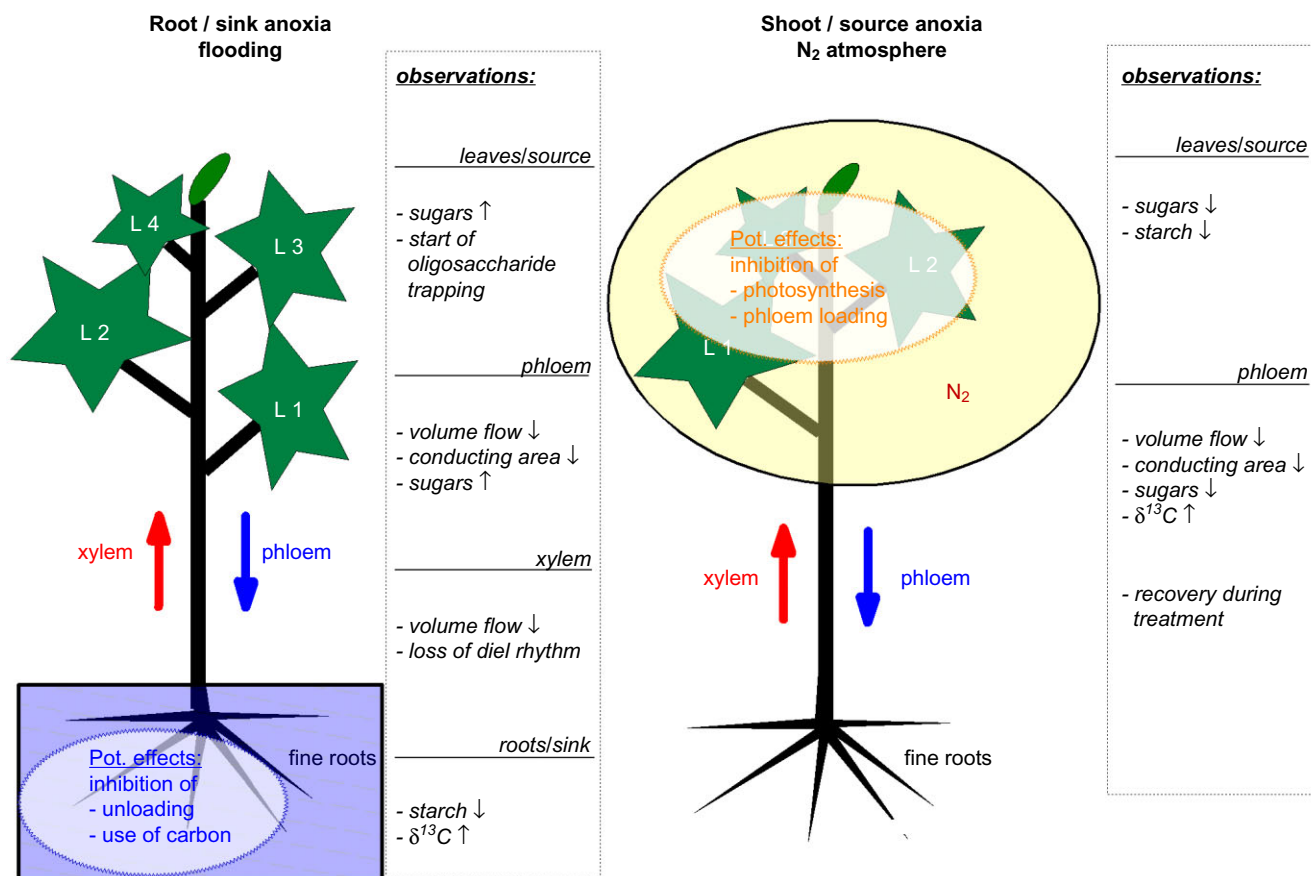


Figure 8. Potential effects and observed changes in carbohydrates and transport parameters at leaves (source), phloem, xylem and roots (sinks) in *Ricinus* after exposing the sink (root) for 3 d or source (shoot) for 3 h to anoxia.

processes were affected by the present treatments like, for example, photosynthesis or growth.

It is very likely that the present anoxic treatments do not have only primary effects on phloem flow. Under flooding, the carbohydrates cannot be efficiently used in roots and, in addition, toxic substances created during fermentation may be transported via xylem to the leaves. Under shoot anoxia, the loading of actual photoassimilates was interrupted and shifted to the use of stored starch. For phloem loading, apparently enough energy was available.

ACKNOWLEDGMENTS

We thank Karl Merz, Forest Botanical Garden, Freiburg, for technical support during plant cultivation. A.D.P. thanks the European Commission (RITA-026164, proposal # WNMRC06-002) for financial support. A.G. acknowledges support from the German Research Council (DFG) under contract numbers GE 1090/8-1 and 9-1.

REFERENCES

Angelov M.N., Sung S.J., Doong R.L., Harms W.R., Kormanik P.P. & Black J.C. (1996) Long- and short-term flooding effects on survival and sink–source relationships of swamp-adapted tree species. *Tree Physiology* **16**, 477–484.

- Bailey-Serres J. & Voesenek L.A.C.J. (2008) Flooding stress: acclimations and genetic diversity. *Annual Review of Plant Biology* **59**, 313–339.
- van Bel A.J.E. (1993) The transport phloem. Specifics of its functioning. *Progress in Botany* **54**, 134–150.
- van Bel A.J.E. (2003) The phloem, a miracle of ingenuity. *Plant, Cell & Environment* **26**, 125–149.
- van Bel A.J.E. & Kempers R. (1990) Symplastic isolation of the sieve element-companion cell complex in the phloem of *Ricinus communis* and *Salix alba* stems. *Planta* **183**, 69–76.
- Borisjuk L., Rolletschek H. & Neuberger T. (2012) Surveying the plant's world by magnetic resonance imaging. *The Plant Journal* **70**, 129–146.
- Brandes E., Kodama N., Whittaker K., Weston C., Rennenberg H., Keitel C., ... Gessler A. (2006) Short-term variation in the isotopic composition of organic matter allocated from the leaves to the stem of *Pinus sylvestris*: effects of photosynthetic and postphotosynthetic carbon isotope fractionation. *Global Change Biology* **12**, 1922–1939.
- De Schepper V., De Swaef T., Bauweraerts I. & Steppe K. (2013) Phloem transport: a review of mechanisms and controls. *Journal of Experimental Botany* **64**, 4839–4850.
- van Dongen J.T., Schurr U., Pfister M. & Geigenberger P. (2003) Phloem metabolism and function have to cope with low internal oxygen. *Plant Physiology* **131**, 1529–1543.
- Donker H.C.W. & Van As H. (1999) Cell water balance of white button mushrooms (*Agaricus bisporus*) during its post-harvest lifetime studied by quantitative magnetic resonance imaging. *Biochimica et Biophysica Acta* **1427**, 287–297.
- Donker H.C.W., Van As H., Snijder H.J. & Edzes H.T. (1997) Quantitative ^1H -NMR imaging of water in white button mushrooms (*Agaricus bisporus*). *Magnetic Resonance Imaging* **15**, 113–121.
- Edzes H.T., van Dusschoten D. & Van As H. (1998) Quantitative T2 imaging of plant tissues by means of multi-echo MRI microscopy. *Magnetic Resonance Imaging* **16**, 185–196.

- Else M.A., Coupland D., Dutton L. & Jackson M.B. (2008) Decreased root hydraulic conductivity reduces leaf water potential, initiates stomatal closure and slows leaf expansion in flooded plants of castor oil (*Ricinus communis*) despite diminished delivery of ABA from the roots to shoots in xylem sap. *Physiologia Plantarum* **111**, 46–54.
- Geigenberger P. (2003) Response of plant metabolism to too little oxygen. *Current Opinion in Plant Biology* **6**, 247–256.
- Gessler A., Tcherkez G., Peuke A.D., Ghashghaie J. & Farquhar G. (2008) Experimental evidence for diel variations of the carbon isotope composition in leaf, stem and phloem sap organic matter in *Ricinus communis*. *Plant, Cell & Environment* **31**, 941–953.
- Gharbi I., Ricard B., Smi S., Bizid E. & Brouquisse R. (2009) Increased hexose transport in the roots of tomato plants submitted to prolonged hypoxia. *Planta* **230**, 441–448.
- Gould N., Thorpe M.R., Koroleva O. & Minchin P.E.H. (2005) Phloem hydrostatic pressure relates to solute loading rate: a direct test of the Münch hypothesis. *Functional Plant Biology* **32**, 1019–1026.
- Göttlicher S., Knohl A., Wanek W., Buchmann N. & Richter A. (2006) Short-term changes in carbon isotope composition of soluble carbohydrates and starch: from canopy leaves to the root system. *Rapid Communications in Mass Spectrometry* **20**, 653–660.
- Hall A.J. & Minchin P.E.H. (2013) A closed-form solution for steady-state coupled phloem/xylem flow using the Lambert-W function. *Plant, Cell & Environment* **36**, 2150–2162.
- Jaeger C., Gessler A., Biller S., Rennenberg H. & Kreuzwieser J. (2009) Differences in C metabolism of ash species and provenances as a consequence of root oxygen deprivation by waterlogging. *Journal of Experimental Botany* **60**, 4335–4345.
- Jensen K.H., Lee J., Bohr T., Bruus H., Holbrook N.M. & Zwieniecki M.A. (2011) Optimality of the Münch mechanism for translocation of sugars in plants. *Journal of the Royal Society, Interface* **8**, 1155–1165.
- Jeschke W.D. & Pate J.S. (1991) Modeling of the partitioning, assimilation and storage of nitrate within root and shoot organs of castor bean (*Ricinus communis* L.). *Journal of Experimental Botany* **42**, 1091–1103.
- Keitel C., Matzarakis A., Rennenberg H. & Gessler A. (2006) Carbon isotopic composition and oxygen isotopic enrichment in phloem and total leaf organic matter of European beech (*Fagus sylvatica* L.) along a climate gradient. *Plant, Cell & Environment* **29**, 1492–1507.
- Knoblauch M. & Oparka K. (2012) The structure of the phloem – still more questions than answers. *The Plant Journal* **70**, 147–156.
- Komor E. (2000) Source physiology and assimilate transport: the interaction of sucrose metabolism, starch storage and phloem export in source leaves and the effects on sugar status in phloem. *Australian Journal of Plant Physiology* **27**, 497–505.
- Kreuzwieser J., Hauberg J., Howell K.A., Carroll A., Rennenberg H., Millar A.H. & Whelan J. (2009) Differential response of grey poplar leaves and roots underpins stress adaptation during hypoxia. *Plant Physiology* **149**, 461–473.
- Lalonde S., Tegeder M., Throne-Holst M., Frommer W.B. & Patrick J.W. (2003) Phloem loading and unloading of sugars and amino acids. *Plant, Cell & Environment* **26**, 37–56.
- Lalonde S., Wipf D. & Frommer W.B. (2004) Transport mechanisms for organic forms of carbon and nitrogen between source and sink. *Annual Review of Plant Biology* **55**, 341–372.
- Merchant A., Peuke A.D., Keitel C., McFarlane C., Warren C.R. & Adams M.A. (2010) Phloem sap and leaf $\delta^{13}\text{C}$, carbohydrates, and amino acid concentrations in *Eucalyptus globulus* change systematically according to flooding and water deficit treatment. *Journal of Experimental Botany* **61**, 1785–1793.
- Mullendore D.L., Windt C.W., Van As H. & Knoblauch M. (2010) Sieve tube geometry in relation to phloem flow. *The Plant Cell* **22**, 579–593.
- Münch E. (1930) *Die Stoffbewegungen in der Pflanze*, G. Fischer Verlag, Jena, Germany.
- Narsai R., Rocha M., Geigenberger P., Whelan J. & van Dongen J.T. (2011) Comparative analysis between plant species of transcriptional and metabolic responses to hypoxia. *The New Phytologist* **190**, 472–487.
- Pate J.S., Sharkey P.J. & Lewis O.A.M. (1974) Phloem bleeding from legume fruits – A technique for study of fruit nutrition. *Planta* **120**, 229–243.
- Peuke A.D. (2010) Correlations in concentrations, xylem and phloem flows, and partitioning of elements and ions in intact plants. A summary and statistical re-evaluation of modelling experiments in *Ricinus communis*. *Journal of Experimental Botany* **61**, 635–655.
- Peuke A.D. & Jeschke W.D. (1993) The uptake and flow of C, N and ions between roots and shoots in *Ricinus communis* L. I. Grown with ammonium or nitrate as nitrogen source. *Journal of Experimental Botany* **44**, 1167–1176.
- Peuke A.D., Rokitta M., Zimmermann U., Schreiber L. & Haase A. (2001) Simultaneous measurement of water flow velocity and solute transport in xylem and phloem of adult plants of *Ricinus communis* during day time course by nuclear magnetic resonance (NMR) spectrometry. *Plant, Cell & Environment* **24**, 491–503.
- Peuke A.D., Windt C. & Van As H. (2006) Effects of cold-girdling on flows in the transport phloem in *Ricinus communis*: is mass flow inhibited? *Plant, Cell & Environment* **29**, 15–25.
- Pickard W.F. & Abraham-Shrauner B. (2009) A 'simplest' steady-state Münch-like model of phloem translocation, with source and pathway and sink. *Functional Plant Biology* **36**, 629–644.
- Rennie E.A. & Turgeon R. (2009) A comprehensive picture of phloem loading strategies. *Proceedings of the National Academy of Sciences of the United States of America* **106**, 14162–14167.
- Richter A., Wanek W., Werner R.A., Ghashghaie J., Jaggi M., Gessler A., . . . Gleixner G. (2009) Preparation of starch and soluble sugars of plant material for the analysis of carbon isotope composition: a comparison of methods. *Rapid Communications in Mass Spectrometry* **23**, 2476–2488.
- Scheenen T.W., van Dusschoten D., De Jager P.A. & Van As H. (2000a) Microscopic displacement imaging with pulsed field gradient turbo spin-echo NMR. *Journal of Magnetic Resonance* **142**, 207–215.
- Scheenen T.W., Vergeldt F.J., Windt C.W., de Jager P.A. & Van As H. (2001) Microscopic imaging of slow flow and diffusion: a pulsed field gradient stimulated echo sequence combined with turbo spin echo imaging. *Journal of Magnetic Resonance* **151**, 94–100.
- Scheenen T.W.J., van Dusschoten D., de Jager P.A. & Van As H. (2000b) Quantification of water transport in plants with NMR imaging. *Journal of Experimental Botany* **51**, 1751–1759.
- Shabala S. (2011) Physiological and cellular aspects of phytotoxicity tolerance in plants: the role of membrane transporters and implications for crop breeding for waterlogging tolerance. *The New Phytologist* **190**, 289–298.
- Slewinski T.L. & Braun D.M. (2010) Current perspectives on the regulation of whole-plant carbohydrate partitioning. *Plant Science* **178**, 341–349.
- Tadege M., Dupuis I. & Kuhlemeier C. (1999) Ethanol fermentation: new functions for an old pathway. *Trends in Plant Science* **4**, 320–325.
- Thompson M.V. & Holbrook N.M. (2003) Application of a single-solute non-steady-state phloem model to the study of long-distance assimilate transport. *Journal of Theoretical Biology* **220**, 419–455.
- Thorpe M.R. & Minchin P.E.H. (1987) Effects of anoxia on phloem loading in C3 and C4 species. *Journal of Experimental Botany* **38**, 221–232.
- Tournaire-Roux C., Sutka M., Javot H., Gout E., Gerbeau P., Luu D.-T., . . . Maurel C. (2003) Cytosolic pH regulates root water transport during anoxic stress through gating of aquaporins. *Nature* **425**, 393–397.
- Turgeon R. (1987) Phloem unloading in tobacco sink leaves: insensitivity to anoxia indicates a symplastic pathway. *Planta* **171**, 73–81.
- Turgeon R. (2010) The role of phloem loading reconsidered. *Plant Physiology* **152**, 1817–1823.
- Turnbull C.G. & Lopez-Cobollo R.M. (2013) Heavy traffic in the fast lane: long-distance signalling by macromolecules. *The New Phytologist* **198**, 33–51.
- Van As H. (2007) Intact plant MRI for the study of cell water relations, membrane permeability, cell-to-cell and long distance water transport. *Journal of Experimental Botany* **58**, 743–756.
- Vu J.C.V. & Yelenosky G. (1991) Photosynthetic responses of citrus trees to soil flooding. *Physiologia Plantarum* **81**, 7–14.
- Wanek W., Heintel S. & Richter A. (2001) Preparation of starch and other carbon fractions from higher plant leaves for stable carbon isotope analysis. *Rapid Communications in Mass Spectrometry* **15**, 1136–1140.
- van der Weerd L., Claessens M.M.A.E., Efte C. & Van As H. (2002) Nuclear magnetic resonance imaging of membrane permeability changes in plants during osmotic stress. *Plant, Cell & Environment* **25**, 1539–1549.
- Windt C.W., Vergeldt F.J., De Jager P.A. & Van As H. (2006) MRI of long-distance water transport: a comparison of the phloem and xylem flow characteristics and dynamics in poplar, castor bean, tomato and tobacco. *Plant, Cell & Environment* **29**, 1715–1729.

Received 25 April 2014; received in revised form 25 June 2014; accepted for publication 27 June 2014